FEBS Letters 585 (2011) 737–743

FEBS Letters
journal homepage: www.FEBSLetters.org

NDUFB7 and NDUFA8 are located at the intermembrane surface of complex I

Radek Szklarczyk [a,1], Bas F.J. Wanschers [a,b,1], Sander B. Nabuurs [a], Jessica Nouws [b], Leo G. Nijtmans [b], Martijn A. Huynen [a,*]

[a] Centre for Molecular and Biomolecular Informatics, Radboud University Nijmegen Medical Centre, 6500 HB, Nijmegen, The Netherlands
[b] Nijmegen Centre for Mitochondrial Disorders at the Department of Pediatrics, Radboud University Nijmegen Medical Centre, 6500 HB, Nijmegen, The Netherlands

ARTICLE INFO

Article history:
Received 24 December 2010
Revised 21 January 2011
Accepted 31 January 2011
Available online 22 February 2011

Edited by Peter Brzezinski

Keywords:
Mitochondria
Complex I
Sequence conservation
Disulfide bridge
Protein localization

ABSTRACT

Complex I (NADH:ubiquinone oxidoreductase) is the first and largest protein complex of the oxidative phosphorylation. Crystal structures have elucidated the positions of most subunits of bacterial evolutionary origin in the complex, but the positions of the eukaryotic subunits are unknown. Based on the analysis of sequence conservation we propose intra-molecular disulfide bridges and the inter-membrane space localization of three Cx_9C-containing subunits in human: NDUFS5, NDUFB7 and NDUFA8. We experimentally confirm the localization of the latter two, while our data are consistent with disulfide bridges in NDUFA8. We propose these subunits stabilize the membrane domain of complex I.

Structured summary: **NDUFA8** and **NDUFS3** physically interact by blue native page (View interaction)

1. Introduction

The NADH:ubiquinone oxidoreductase (complex I) catalyzes the first step of the oxidative phosphorylation and consists of 45 proteins in human. Embedded in the mitochondrial inner membrane, it couples the oxidation of NADH to the reduction of ubiquinone and the translocation of protons across the inner membrane. Given its size and role in energy conversion it is not surprising that complex I deficiencies are the most frequently encountered class of mitochondrial disorders [1,2].

The mitochondrial complex I originated from a 14–17 subunit bacterial complex [3]. In the eukaryotes the complex gained 25–30 subunits that are not present in bacteria (so-called "supernumerary subunits") [4]. The supernumerary subunits contribute 32% of the complex' molecular mass in human. In bacteria, the complex is active without the additional subunits, and the increased size and complexity of the enzyme as well as the function of supernumerary subunits in eukaryotes represent a puzzle. It has been hypothesized that the eukaryotic subunits assist in the biogenesis and support stability of the mitochondrial complex [5].

In the mitochondrial inter-membrane space (IMS) reside two families of short proteins that include repeated double cysteine motifs (Cx_9C or Cx_3C). The cysteines are oxidized in the IMS, forming disulfide bridges that stabilize a hairpin confirmation in which α-helices between the cysteines align in an anti-parallel manner [6–10] (Fig. 1). The oxidation of the cysteines is catalyzed by the MIA40/ERV1 disulfide bond relay that resides in the IMS [11–13]. The regularly spaced cysteines have been shown to be essential for the IMS localization [14]. Mature proteins become trapped in the IMS, with the disulfide bonds preventing membrane translocation [15]. Here we analyze three supernumerary subunits of complex I to show that they also contain Cx_9C domains and are in all likelihood located at the IMS surface of complex I. Experimental analyses of the localization of two of the subunits and the timing of assembly of one of the subunits are in agreement with this prediction.

2. Results

2.1. NDUFS5, NDUFB7 and NDUFA8 contain Cx_9C domains

Complex I consists of multiple proteins with conserved cysteines, a number of which are involved in Fe–S cluster binding. Nevertheless, for NDUFS5 (16kD subunit, PFFD), NDUFB7 (B18 subunit) and NDUFA8 (19kD subunit, PGIV) no Fe–S cluster binding has been observed [5,16]. Instead they exhibit a number of features typical of Cx_9C domains (see Table 1 and Fig. 1). The proteins are

* Corresponding author. Address: CMBI 260, NCMLS, Radboud University Nijmegen Medical Centre, P.O. Box 9101, 6500 HB Nijmegen, The Netherlands. Fax: +31 24 3619395.
E-mail address: huynen@cmbi.ru.nl (M.A. Huynen).
[1] Contributed equally.

0014-5793/$36.00 © 2011 Federation of European Biochemical Societies. Published by Elsevier B.V. All rights reserved.
doi:10.1016/j.febslet.2011.01.046

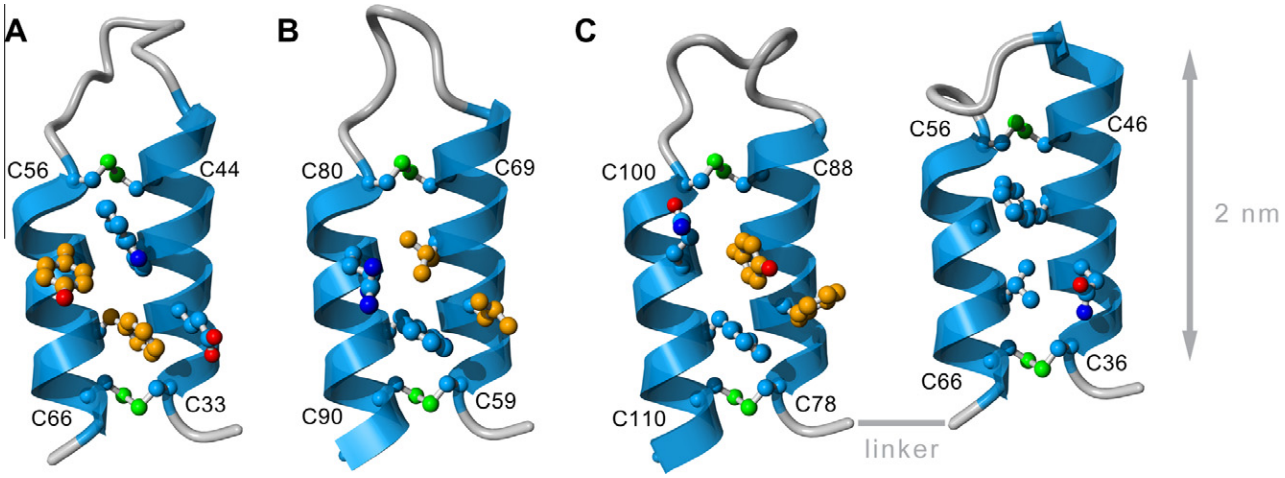

Fig. 1. Molecular models of the Cx_9C domains of NDUFS5, NDUFB7 and NDUFA8. Homology models are shown for the helical hairpins of (A) NDUFS5, (B) NDUFB7 and (C) NDUFA8. The position of the linker between the two Cx_9C domains of NDUFA8 is indicated. For all models, the bridged cysteine side chains involved in stabilizing the helical hairpin structure are shown and labeled. Additionally, the amino acids located at the 4th and 7th position of each Cx_9C motif are also shown. Amino acid side chains at these positions matching the IMS targeting signal consensus sequence [17] are depicted (orange).

Table 1
Features characteristic to NDUFS5, NDUFB7 and NDIFA8 and to the Fe–S binding central subunit NDUFV2. Columns denote: the size of proteins in amino acids in human; the form of the Cx_9C domain (conserved in all eukaryotes); distance between the motifs that corresponds to the loop of the hairpin; overlap between the motifs and (predicted) α helices; presence of a cleaved N-terminal import signal; conservation pattern for the domain, 4th and 7th positions of constrained variation are marked with a star.[1]) See the Supplementary data for the list of human Cx_9C domain proteins.

	Size	Cys domain	Distance between Cys motifs	CxC in α-helices	Cleaved targeting presequence	Localization	Conservation pattern
NDUFS5	106	Twin Cx_9C	12	Yes	No	Membrane arm of CI	
NDUFB7	137	Twin Cx_9C	10	Yes	No	Membrane arm of CI	
NDUFA8	172	Quadruple Cx_9C	9–11, 10–11	Yes	No	Membrane arm of CI	
Other human IMS Cx_9C proteins[1]	63–227	Twin Cx_9C; Twin Cx_3C	5–22	Yes	No	IMS	(COX17)
NDUFV2 (Fe-S)	250	Cx_3C, Cx_4C	35	No	Yes	Matrix	

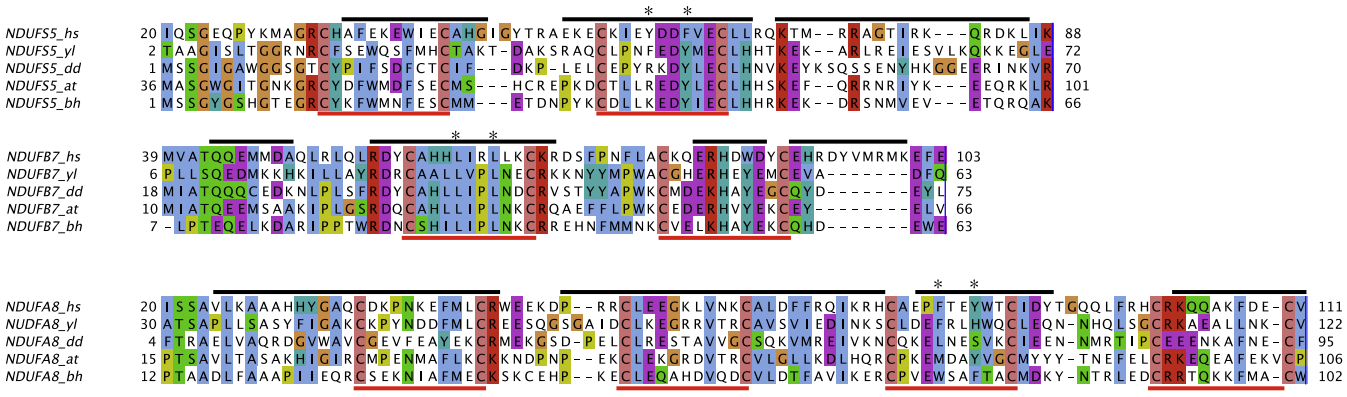

Fig. 2. Alignments of Cx_9C domain-containing NDUFS5, NDUFB7, NDUFA8. Twin Cx_9C motifs are indicated under the alignment (red line) and predicted (Jpred3, [45]) α-helices (black) are indicated above the sequences. Stars mark the localization of the IMS targeting signal in the human sequences. The NDUFA8 gene for *B. hominis* was predicted from the DNA (see Supplementary data). Abbreviations: hs, *Homo sapiens*; yl, *Y. lipolytica*; dd, *Dictyostelium discoideum*; at, *Arabidopsis thaliana*; bh, *B. hominis*.

Table 2
Presence/absence pattern of Cx_9C domain-containing genes in respiratory chain complexes among eukaryotes. Major eukaryotic supergroups [46] are listed in the top row. The proteins are entirely absent in species that do not posses the canonical form of mitochondria (*i.e.*, species that miss respiratory chain-containing organelles and mtDNA, white-on-black typeface). Not all of the remaining Cx_9C domain-containing proteins are conserved in aerobic species (grey).

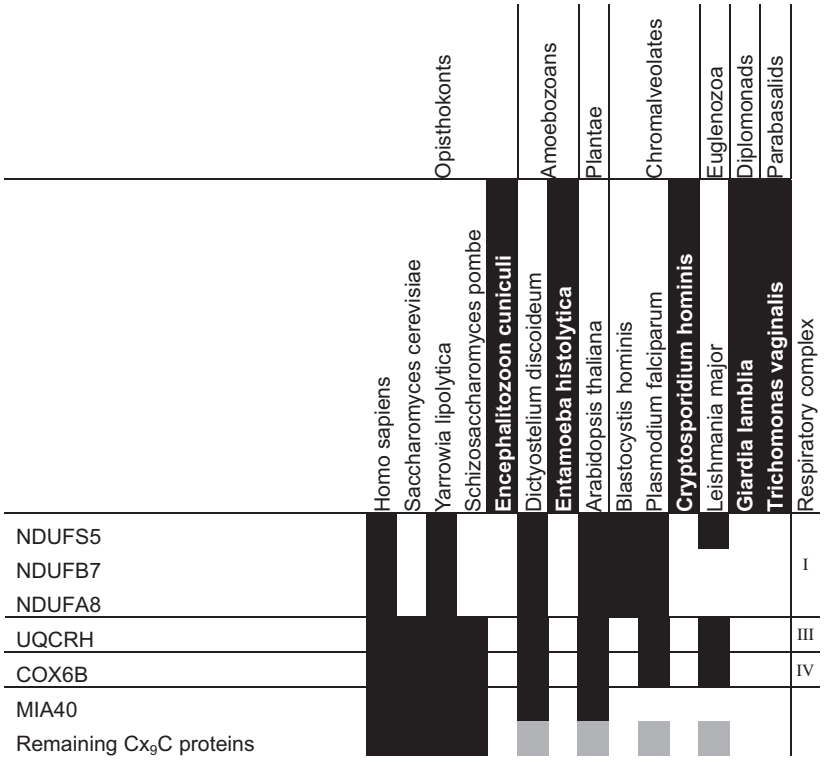

generally small (<230 amino acids). The distance between the Cx_9C motifs, corresponding to the loop linking the two α-helices, is usually short (5–22 residues). Secondary structure predictions for the three CI subunits indicate that the Cx_9C motifs form α-helices (Fig. 2), akin to Cx_9C domain-containing proteins with known structure (for example [6]). The residues at the 4th and 7th positions of the motif form the inter-membrane space targeting signal [17,18] (Fig. 1), as well as constitute the hydrophobic core of the Cx_9C domain in the Mia40 folding pathway [19].

Multiple yeast Cx_9C proteins are functionally linked to respiratory chain complexes [7]. The phylogenetic distribution of Cx_9C domain-containing proteins (Table 2) shows their evolutionary association with aerobic eukaryotes that posses a canonical form of mitochondria as well as the proteins' association with respiratory chain complexes I, III and IV. Almost all Cx_9C domain-containing proteins can be found in species that also posses complex III and complex IV. By contrast, the three Cx_9C complex I subunits strictly co-occur with complex I, and are the only proteins with this domain encoded in the *Blastocystis hominis* genome that lacks complex III and complex IV (Table 2).

2.2. Intramolecular disulfide bridges in complex I subunits

Many posttranslational modifications have been reported for proteins that constitute complex I, including Fe–S clusters, phosphorylation, acetylation, S-nitrosylation, and the cleavage of N-terminal targeting sequences (see [20] for review). Intramolecular cross-linking has not been reported for mammalian complex I subunits to date. However, the *Neurospora crassa* ortholog of NDUFA8 has been inferred to contain intramolecular disulfide bonds [21]. To test whether human NDUFA8 (that contains two twin Cx_9C domains) forms disulfide bridges, mitochondria with disrupted outer membranes (mitoplasts) were isolated and proteins were analyzed for their electrophoretic behavior in the presence or absence of a reducing agent (2-mercaptoethanol) using SDS–PAGE. An NDUFA8-specific antibody shows a slower migrating band under reducing conditions compared to non-reducing conditions (Fig. 3A, upper panel). A slower migration suggests a change in the protein structure in reduced versus non-reduced conditions. To rule out migration artefacts introduced by the electrophoresis in reduced conditions, the membrane was reprobed with an antibody against cyclophilin B (a protein that does not contain intra-molecular disulfide bridges). No difference in migration of cyclophilin B was observed (Fig. 3A, lower panel). Similar results were obtained for NDUFA8-Myc-His, however, a reducing environment did not alter the migration pattern of Myc-His-tagged NDUFB7 protein (data not shown), possibly because of the presence of only one predicted Cx_9C domain in this protein compared to two Cx_9C domains in NDUFA8, and therewith a more limited effect on the protein conformation. NDUFS5-Myc-His transgene expression did not reach detectable levels (see Section 4).

2.3. Localization of NDUFS5, NDUFB7 and NDUFA8

In agreement with other Cx_9C proteins, the three complex I subunits do not have a cleaved targeting sequence [5]. Additionally, all three subunits contain an intermembrane space targeting signal, which is found in all known and predicted Mia40 substrates [18]. The presence of a Cx_9C domain with the IMS targeting signal (Fig. 1) and the absence of a canonical mitochondrial targeting signal suggest the insertion of the three subunits into the complex directly from the IMS. Experiments involving mild detergents

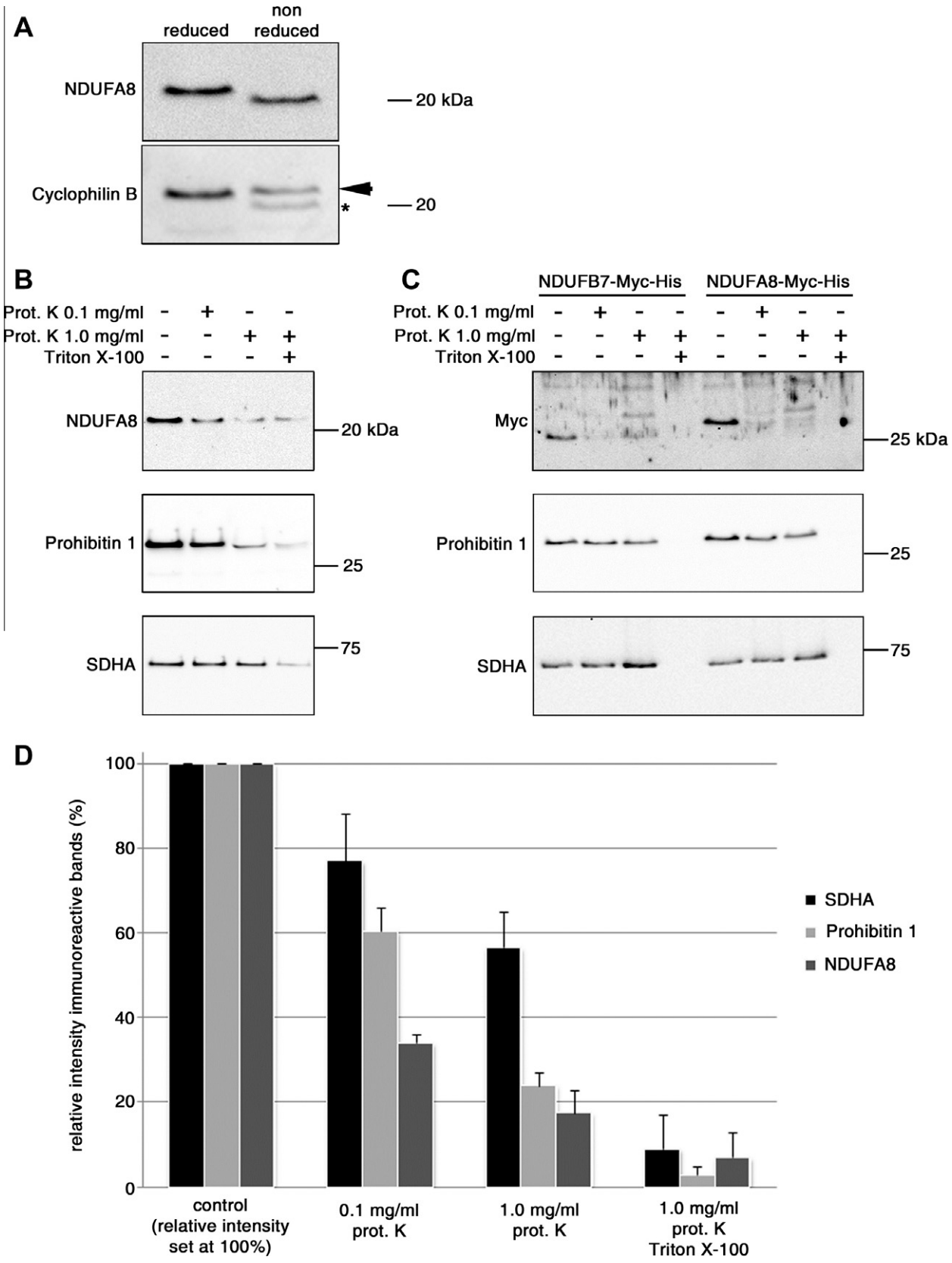

Fig. 3. NDUFA8 forms intramolecular disulfide bridges and, together with NDUFB7, is localized in the mitochondrial inter membrane space. (A) Electrophoretic analysis of NDUFA8 under reducing and non-reducing conditions (with or without 2-mercaptoethanol). NDUFA8 (upper panel) and the negative control cylophilin B (lower panel) were analyzed with specific antibodies. The arrowhead indicates the cyclophilin-B signal, the asterisk denotes the NDUFA8 signal from the previous incubation. (B) Western blot analysis of NDUFA8 and (C) NDUFA8–NDUFB7-Myc-His from mitochondria without the outer membrane (mitoplasts) following proteinase K protection assay. Mitoplasts (lanes 1, 5) were treated with proteinase K (concentrations 0.1 and 1.0 mg/ml, lanes 2, 6 and 3, 7) and inner-membrane dissolving Triton X-100 (lanes 4 and 8). Sensitivity of NDUFA8 and Myc-His tagged NDUFB7 and NDUFA8 for proteinase K (upper panels) was analyzed. The IMS protein prohibitin 1 is shown in the middle panels, above the matrix localized SDHA. (D) Quantification of the immunoreactive bands from B and a repeated experiment.

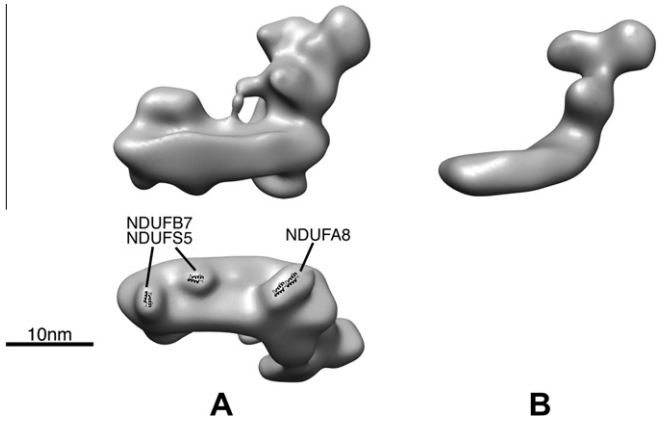

Fig. 4. Electron microscopy model of complex I in eukaryotes and bacteria. (A) Hypothetical positions of Cx_9C domain-containing subunits in the structure of bovine complex I. Cx_9C domain is shown to scale (the length of the α-helix is around 2 nm, as shown in Fig. 1). NDUFA8 that contains two Cx_9C domains can be recognized based on the larger size of the protrusion and from being a part of the Iα subcomplex together with the matrix arm [5]. Based on the existing data, it is not possible to unambiguously assign NDUFB7 and NDUFS5 to the other protrusions. (B) Bacterial complex I from *Aquifex aeolicus*, shown to scale. Electron microscopy models are reproduced with permission from [25].

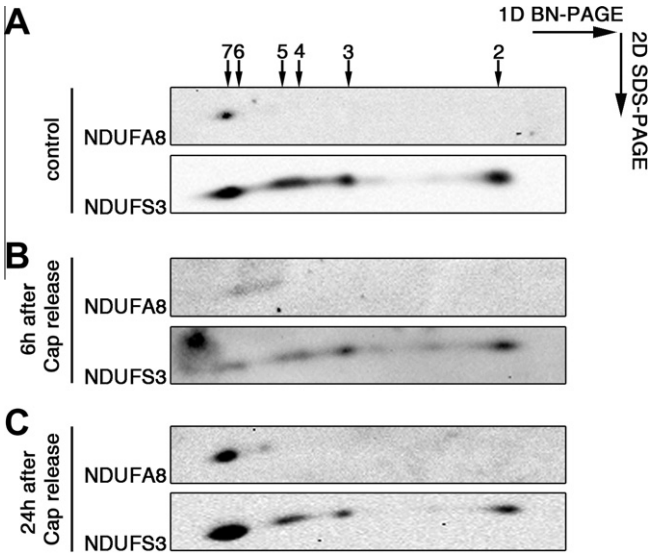

Fig. 5. Two-dimensional blue native PAGE analysis of NDUFA8. HEK293 cells were cultured for 3 days in the absence (control, A) or presence of chloramphenicol that inhibits the mitochondrial translation. The translation was allowed to resume again for 6 hours (B) and 24 h (C) after removal of the chloramphenicol before harvest. Subsequently, 2D SDS–PAGE and Western blotting were carried out and the membranes were probed with antibodies against NDUFA8 and NDUFS3. Indicated with arrows are subcomplexes 3–6 and the NDUFS3 monomer (m) [29]. The holocomplex is denoted with 7.

indicate that the three complex I subunits co-localize with membrane subunits of complex I [22]. However, the three subunits do not contain transmembrane domains. This parallels the two other subunits of respiratory chain complexes that contain Cx_9C domains, UQCRH and COX6B. These reside in the aqueous IMS, while being part of membrane-embedded complexes [23,24].

The recent bovine complex I structure determined by 3D electron microscopy [25] reveals three IMS protrusions in its membrane arm, with two larger protrusions present in *Yarrowia lipolytica* [26]. The predicted sizes of the hairpin-folded Cx_9C domain-containing complex I subunits, as shown in Fig. 1, would fit within these protrusions (see Fig. 4A), with NDUFA8 fitting in the largest protrusion, close to the "heel" of the complex and consistent with its addition to subcomplexes 5 and 6 in the assembly assay (see below). The protrusions are absent in the bacterial complex I structure ([25] and Fig. 4B), consistent with the absence of Cx_9C domain homologs in bacteria.

To verify the predicted IMS localization of NDUFA8 and NDUFB7, a proteinase K protection assay was carried out on mitochondria without the outer membrane. A substantial fraction of the endogenous NDUFA8, as well as the IMS protein prohibitin 1, was digested by proteinase K (Fig. 3B). In contrast, SDHA, a mitochondrial matrix localized subunit of complex II was degraded only upon dissolving the inner membrane (Fig. 3B and D). Additionally, the proteinase K protection assay was repeated using cells expressing Myc-His tagged NDUFA8 and NDUFB7, showing efficient tag digestion at low proteinase K concentrations (Fig. 3C). Thus, the experimental data support the IMS localization of NDUFA8 and NDUFB7.

2.4. NDUFA8. is added to the complex I in its final assembly stages

Disulfide bonds are present in the soluble *N. crassa* ortholog of NDUFA8 as well as in the assembled subunit [21] suggesting that the formation of disulfide bridges precedes IMS insertion into the complex, and that the Cx_9C domain-containing proteins are assembled into complex I directly from the IMS. This, in turn, implies that the Cx_9C domain-containing proteins will be added relatively late in assembly, when a partial complex has already been inserted into the membrane. Indeed, NDUFS5 has been found to be incorporated into the holocomplex at a late assembly stage, and is not found in complex I assembly intermediates [22], similar to the late insertion of COX6b into complex IV [27,28]. We tested the hypothesis that Cx_9C domain-containing proteins are added late to the complex from the IMS for NDUFA8. To trace the complex I assembly process, mitochondrial translation was inhibited with chloramphenicol for three days after which the translation was allowed to resume. The presence of the matrix subunit NDUFS3 and the Cx_9C domain-containing NDUFA8 were examined with 2D BN-PAGE analysis (Fig. 5). Upon normal mitochondrial translation NDUFS3 is present in multiple sub-complexes (listed in [29]), while the Cx_9C domain-containing NDUFA8 is detectable only in the holocomplex (Fig. 5A). Due to the complex I turnover, after prolonged inhibited translation the holocomplex becomes undetectable (data not shown). Consistent with the prediction, six hours after resuming the translation (Fig. 5B) NDUFA8 becomes detectable in late stages of assembly, when the complex is embedded in the inner membrane (sub-complexes 5 and 6 [29]), while NDUFS3 can be detected in partially formed sub-complexes. After 24 h NDUFA8 becomes detectable in the membrane-bound holocomplex (Fig. 5C).

3. Discussion

The cysteine-rich complex I subunits of eukaryotic origin have been proposed to play role in binding and assembly of Fe–S clusters [21,30,31]. Recognition of Cx_9C domains in NDUFS5, NDUFB7, NDUFA8 (see also [30]), together with identification of domains' defining features allow us to predict and test subunits' localization and assembly in complex I.

The recent X-ray crystallography analysis of the complete *Y. lipolytica* complex [16] does not show Fe–S clusters in the membrane arm of complex I. Additionally, despite the strict evolutionary co-occurrence with complex I (Table 2), our molecular modeling studies show that the nine residue cysteine spacing does not appear to be in a configuration that would allow metal binding, and the sequence conservation pattern is markedly different from Fe–S binding centers of complex I (see Table 1). This makes a role of the Cx_9C domain in the Fe–S delivery or assembly unlikely. The

Cx_9C domain in other IMS proteins is responsible for the formation and stabilization of the hairpin structure, precluding membrane translocation and trapping proteins in the IMS [15]. Furthermore, the late incorporation of Cx_9C proteins in the already membrane-embedded complex I supports the IMS localization. The late addition of NDUFA8 to the complex, consistent with similar observations for NDUFS5 [22], points to the stabilizing role of the disulfide-bound Cx_9C subunits rather than their involvement in the assembly process.

COX6b plays a structural role in complex IV, and is responsible for its dimerization [23]. A structural role for the Cx_9C domains in complex I would be consistent with the *N. crassa* NDUFS5 and NDUFA8 deletion phenotypes that prevent the full assembly of complex I, as well as lead to the accumulation of membrane arm intermediates, suggesting the proteins' importance for stability and biogenesis of the complex [32,33]. Therefore we postulate a structural role of Cx_9C domains in complex I. Stabilization of the membrane arm from the IMS is a functionality that might have been necessary for the eukaryotic complex I, which increased its subunit count since the acquisition of the α-proteobacterial endosymbiont. Irrespective of the specific role of the Cx_9C domain-proteins in complex I, their presence within the complex suggests an explanation why complex IV is required for stability of complex I [34]. The oxidation of the Cx_9C domain-containing proteins depends on the functioning of complex IV via the MIA40/ERV1 disulfide relay system [35].

4. Methods

4.1. Cloning and stable cell line generation

The NDUFS5 and NDUFA8 gene were PCR-amplified and cloned in a mammalian expression vector adding a Myc-His tag at the C-terminus using the Gateway system (Invitrogen, see Supplementary data for details). The NDUFB7 clone (HsCD00040509) was ordered from The Plasmid Information database [36]. Human Embryonic Kidney (HEK) 293 and HEK293 T-REx™ Flp-In™ cells were maintained at standard culture conditions. HEK293 T-REx™ Flp-In™ cells were subsequently transfected with the appropriate expression vector using Superfect (Qiagen) to generate stable NDUFS5-, NDUFA8- and NDUFB7-Myc-His expressing cells (see Supplementary data for details). Transgene expression induced by doxycycline was sufficient for NDUFA8-Myc-His and NDUFB7-Myc-His, whereas NDUFS5-Myc-His expression was too low to allow further experimental validation.

4.2. Isolation of mitochondrial membranes under reducing conditions

To determine the presence of the predicted intramolecular disulfide bridges in NDUFA8 and NDUFB7, mitochondrial membranes were isolated [37]. Samples were diluted once with 2xTricine sample buffer (Biorad) under reducing or non-reducing conditions, *i.e.*, sample buffer with or without 5% [v/v] 2-mercaptoethanol added respectively, incubated for 60 min at room temperature and subjected to sodium dodecyl sulfate polyacrylamide gel electrophoresis (SDS–PAGE) in a 16% gel. Proteins were analyzed by Western blotting and by probing with protein-specific (NDUFA8) and tag-specific (Myc) antibodies (see Supplementary data).

4.3. Cellular fractionation and proteinase K protection assay

Cellular fractionation was done as described before [38]. Next, mitoplasts were generated by permeabilizing the outer membrane of the mitochondria [39]. Susceptibility of proteins to degradation by proteinase K was analyzed after SDS–PAGE and Western blotting with antibodies. The protein concentrations were determined with the micro BCA protein assay kit (Thermo Scientific). Prohibitin 1 upon proteinase K treatment exhibits only a minor decrease (15%, Fig. 3C, middle panel, lane 2 and 3) compared to Myc-tagged complex I subunits (See also Supplementary Fig. 1). This may be an artifact introduced by differences in protein loading (not present in Fig. 3B), visible for SDHA (200% increase, Fig. 3C, lower panel, lane 3) and more abundant background bands detected with the anti-Myc antibody (Fig. 3C, top panel, lane 3). Also, larger amounts of proteinase K are necessary to fully digest the protein (Fig. 3D 1.0 mg/ml). Differences in the efficiency of prohibitin 1 degradation and the necessity for higher concentrations of proteinase K can be attributed to the poor availability of this protein to proteinase K digestion due to its tight folding [40] compared to the Myc tag. Quantifying intensity of immunoreactive bands was performed with the Image Lab software (Biorad).

4.4. 2D blue native polyacrylamide gel electrophoresis

One and two dimensional Blue Native PAGE was done as described previously [22]. For this analysis 80 μg of protein was loaded.

4.5. Molecular modeling of NDUFS5, NDUFB7 and NDUFA8

Homology models of the Cx_9C domains of NDUFS5, NDUFB7 and NDUFA8 were built using the YASARA molecular modeling program [41]. The crystal structure of yeast Mia40 solved at 2.5 Å resolution [42] was used as the modeling template. Prior to model building, the Cx_9C domain was extracted from this complex structure and used as a custom template. The alignment of the four Cx_9C domains of NDUFS5, NDUFB7 and NDUFA8 to the Mia40 Cx_9C sequence was straightforward due to the presence of the four conserved equidistant cysteines in all sequences. Based on the recently proposed mechanism of the Mia40 induced folding pathway for Cx_9C domains [19], and the coevolution of cysteine pairs in NDUFA8 proteins (correlated loss of cysteines C46 and C56 in *Hydra magnipapillata*, *Caenorhabditis elegans* and *Brugia malayi*) the disulfide bridge topology was predicted to be as shown in Fig. 1, rather than a topology in which the first helix interacts with the fourth helix and the second one interacts with the third. Loops were modeled by scanning a non-redundant subset of the PDB for fragments with matching anchor points, a minimal number of bumps, and maximal sequence similarity. Side chains were added with YASARA's implementation of SCWRL [43], and then the model was subjected to an energy minimization with the YASARA2 force field [44]. PDB files of the homology models are available from the authors upon request.

Author's contributions

RS designed the study, carried out the bioinformatics analyses and drafted the manuscript. BFJW performed the experimental work with the help of JN. SBN computed homology models. LGN and MAH supervised the project. All authors read and approved the manuscript.

Acknowledgments

We would like to thank Rinske van de Vorstenbosch and Fenna Hensen for the generous gift of the anti-Myc antibody 9E10 and Hans Spelbrink for advice on the proteinase K protection assay. Herman Swarts for performing the PCRs and initial cloning of NDUFS5 and NDUFA8 and Mariël van den Brand for maintaining

cell culture. We would also like to thank Philip Kensche and Thomas Cuypers for inspiring discussions as well as Michael Radermacher for sharing electron microscopy models of complex I. R.S. and B.F.J.W. are supported by Horizon grant (050-71-053) and S.B.N. is supported by VENI grant (700.58.410) from the Netherlands Organization for Scientific Research (NWO).

Appendix A. Supplementary data

Supplementary data associated with this article can be found, in the online version, at doi:10.1016/j.febslet.2011.01.046.

References

[1] Janssen, R.J.R.J., Nijtmans, L.G., van den Heuvel, L.P. and Smeitink, J.A.M. (2006) Mitochondrial complex I: structure, function and pathology. J. Inherit. Metab. Dis. 29 (4), 499–515.
[2] Distelmaier, F. et al. (2009) Mitochondrial complex I deficiency: from organelle dysfunction to clinical disease. Brain: J. Neurol. 132 (4), 833–842.
[3] Yip, C., Harbour, M.E., Jayawardena, K., Fearnley, I.M. and Sazanov, L.A. (2010) Evolution of respiratory complex I: 'supernumerary' subunits are present in the alpha-proteobacterial enzyme. J. Biol. Chem. 2, 9.
[4] Gabaldón, T., Rainey, D. and Huynen, M.A. (2005) Tracing the evolution of a large protein complex in the eukaryotes, NADH:ubiquinone oxidoreductase (complex I). J. Mol. Biol. 348 (4), 857–870.
[5] Carroll, J., Fearnley, I.M., Shannon, R.J., Hirst, J. and Walker, J.E. (2003) Analysis of the subunit composition of complex I from bovine heart mitochondria,''. Mol Cell Proteom: MCP 2 (2), 117–126.
[6] Arnesano, F., Balatri, E., Banci, L., Bertini, I. and Winge, D.R. (2005) Folding studies of Cox17 reveal an important interplay of cysteine oxidation and copper binding. Structure 13 (5), 713–722.
[7] Longen, S. et al. (2009) Systematic analysis of the twin cx(9)c protein family. J. Mol. Biol. 393 (2), 356–368.
[8] Westerman, B.A., Poutsma, A., Steegers, E.A.P. and Oudejans, C.B.M. (2004) C2360, a nuclear protein expressed in human proliferative cytotrophoblasts, is a representative member of a novel protein family with a conserved coiled coil-helix-coiled coil-helix domain. Genomics 83 (6), 1094–1104.
[9] Banci, L. et al. (2008) A structural-dynamical characterization of human Cox17. J. Biol. Chem. 283 (12), 7912–7920.
[10] Barthe, P. et al. (1997) Solution structure of human p8MTCP1, a cysteine-rich protein encoded by the MTCP1 oncogene, reveals a new alpha-helical assembly motif. J. Mol. Biol. 274 (5), 801–815.
[11] Chacinska, A. et al. (2004) Essential role of Mia40 in import and assembly of mitochondrial intermembrane space proteins. EMBO J. 23 (19), 3735–3746.
[12] Naoé, M. et al. (2004) Identification of Tim40 that mediates protein sorting to the mitochondrial intermembrane space. J. Biol. Chem. 279 (46), 47815–47821.
[13] Mesecke, N. et al. (2005) A disulfide relay system in the intermembrane space of mitochondria that mediates protein import. Cell 121 (7), 1059–1069.
[14] Hofmann, S., Rothbauer, U., Mühlenbein, N., Baiker, K., Hell, K. and Bauer, M.F. (2005) Functional and mutational characterization of human MIA40 acting during import into the mitochondrial intermembrane space. J. Mol. Biol. 353 (3), 517–528.
[15] Herrmann, J.M. and Köhl, R. (2007) Catch me if you can! Oxidative protein trapping in the intermembrane space of mitochondria. J. Cell Biol. 176 (5), 559–563.
[16] Hunte, C., Zickermann, V. and Brandt, U. (2010) Functional modules and structural basis of conformational coupling in mitochondrial complex I. Science (New York, N.Y.).
[17] Sideris, D.P. et al. (2009) A novel intermembrane space-targeting signal docks cysteines onto Mia40 during mitochondrial oxidative folding. J. Cell Biol. 187 (7), 1007–1022.
[18] Milenkovic, D. et al. (2009) Identification of the signal directing Tim9 and Tim10 into the intermembrane space of mitochondria. Mol. Biol. Cell 20 (10), 2530–2539.
[19] Banci, L. et al. (2010) Molecular chaperone function of Mia40 triggers consecutive induced folding steps of the substrate in mitochondrial protein import. Proc. Natl Acad. Sci. USA 107 (47), 20190–20195.
[20] Schilling, B. et al. (2005) Mol. Cell Proteom: MCP 4 (1), 84–96.
[21] Videira, A., Tropschüg, M., Wachter, E., Schneider, H. and Werner, S. (1990) Molecular cloning of subunits of complex I from *Neurospora crassa*. Primary structure and in vitro expression of a 22-kDa polypeptide. J. Biol. Chem. 265 (22), 13060–13065.
[22] Ugalde, C., Vogel, R., Huijbens, R., Van Den Heuvel, B., Smeitink, J. and Nijtmans, L. (2004) Human mitochondrial complex I assembles through the combination of evolutionary conserved modules: a framework to interpret complex I deficiencies. Hum. Mol. Genet. 13 (2461), 2461–2472.
[23] Tsukihara, T. et al. (1996) The whole structure of the 13-subunit oxidized cytochrome c oxidase at 2.8 A. Science (New York, N.Y.) 272 (5265), 1136–1144.
[24] Iwata, S. et al. (1998) Complete structure of the 11-subunit bovine mitochondrial cytochrome bc1 complex. Science (New York, N.Y.) 281 (5373), 64–71.
[25] Clason, T. et al. (2010) The structure of eukaryotic and prokaryotic complex I. J. Struct. Biol. 169 (1), 81–88.
[26] Radermacher, M., Ruiz, T., Clason, T., Benjamin, S., Brandt, U. and Zickermann, V. (2006) The three-dimensional structure of complex I from *Yarrowia lipolytica*: a highly dynamic enzyme. J. Struct. Biol. 154 (3), 269–279.
[27] Nijtmans, L.G., Taanman, J.W., Muijsers, A.O., Speijer, D. and Van den Bogert, C. (1998) Assembly of cytochrome-c oxidase in cultured human cells. Eur. J. Biochem./FEBS 254 (2), 389–394.
[28] Pierrel, F., Khalimonchuk, O., Cobine, P.A., Bestwick, M. and Winge, D.R. (2008) Coa2 is an assembly factor for yeast cytochrome c oxidase biogenesis that facilitates the maturation of Cox1. Mol. Cell. Biol. 28 (16), 4927–4939.
[29] Vogel, R.O. et al. (2007) Identification of mitochondrial complex I assembly intermediates by tracing tagged NDUFS3 demonstrates the entry point of mitochondrial subunits. J. Biol. Chem. 282 (10), 7582–7590.
[30] Cardol, P., Vanrobaeys, F., Devreese, B., Van Beeumen, J., Matagne, R.F. and Remacle, C. (2004) Higher plant-like subunit composition of mitochondrial complex I from *Chlamydomonas reinhardtii*: 31 conserved components among eukaryotes. Biochim. Biophys. Acta 1658 (3), 212–224.
[31] Brandt, U. (2006) Energy converting NADH:quinone oxidoreductase (complex I). Annu. Rev. Biochem. 75, 69–92.
[32] da Silva, M.V. et al. (1996) Disruption of the nuclear gene encoding the 20.8-kDa subunit of NADH: ubiquinone reductase of *Neurospora mitochondria*. Mol. Gen. Genet: MGG 252 (1), 177–183.
[33] Marques, I., Ushakova, A.V., Duarte, M. and Videira, A. (2007) Role of the conserved cysteine residues of the 11.5 kDa subunit in complex I catalytic properties. J. Biochem. 141 (4), 489–493.
[34] Diaz, F., Fukui, H., Garcia, S. and Moraes, C.T. (2006) Cytochrome c oxidase is required for the assembly/stability of respiratory complex I in mouse fibroblasts. Mol. Cell. Biol. 26 (13), 4872–4881.
[35] Hell, K. (2008) The Erv1-Mia40 disulfide relay system in the intermembrane space of mitochondria. Biochim. Biophys. Acta 1783 (4), 601–609.
[36] Zuo, D. et al. (2007) PlasmID: a centralized repository for plasmid clone information and distribution. Nucleic Acids Res. 35, D680–D684.
[37] Nijtmans, L.G.J., Henderson, N.S. and Holt, I.J. (2002) Blue native electrophoresis to study mitochondrial and other protein complexes. Methods (San Diego, Calif.) 26 (4), 327–334.
[38] Vogel, R.O. et al. (2005) Human mitochondrial complex I assembly is mediated by NDUFAF1. FEBS J. 272 (20), 5317–5326.
[39] Duxin, J.P. et al. (2009) Human Dna2 is a nuclear and mitochondrial DNA maintenance protein. Mol. Cell. Biol. 29 (15), 4274–4282.
[40] Nijtmans, L.G.J., Artal, S.M., Grivell, L.A. and Coates, P.J. (2002) The mitochondrial PHB complex: roles in mitochondrial respiratory complex assembly, ageing and degenerative disease. Cell. Mol. Life Sci.: CMLS 59 (1), 143–155.
[41] Krieger, E., Koraimann, G. and Vriend, G. (2002) Increasing the precision of comparative models with YASARA NOVA – a self-parameterizing force field. Proteins 47 (3), 393–402.
[42] Kawano, S. et al. (2009) Structural basis of yeast Tim40/Mia40 as an oxidative translocator in the mitochondrial intermembrane space. Proc. Natl Acad. Sci. USA 106 (34), 14403–14407.
[43] Canutescu, A.A., Shelenkov, A.A. and Dunbrack, R.L. (2003) A graph-theory algorithm for rapid protein side-chain prediction,. Protein Science: A Publication of the Protein Society 12 (9), 2001–2014.
[44] Krieger, E. et al. (2009) Improving physical realism, stereochemistry, and side-chain accuracy in homology modeling: four approaches that performed well in CASP8. Proteins 77, 114–122.
[45] Cole, C., Barber, J.D. and Barton, G.J. (2008) The Jpred 3 secondary structure prediction server. Nucleic Acids Res. 36, W197–201.
[46] Fritz-Laylin, L.K. et al. (2010) The genome of *Naegleria gruberi* illuminates early eukaryotic versatility. Cell 140 (5), 631–642.